Improving the Power Quality and Controllability of PV Power Plants for Microgrids Integration

Luminita Barote, Corneliu Marinescu, Ioan Serban and Daniel Munteanu
Transilvania University of Brasov/Department of Electrical Engineering and Applied Physics
Brasov, Romania
luminita.barote@unitbv.ro

Abstract - **This paper deals with the implementation of the control strategy for a three-phase voltage source inverter (VSI) system with the purpose of improving the power quality and controllability of photovoltaic (PV) system for microgrids (MGs) integration by means of energy storage system. The proposed model comprises of a PV power plant with an energy storage system coupled to the grid by means of a VSI. The PV system and the battery storage are integrated with the help of DC-DC and DC-AC converters in such a way that bidirectional flow of active and reactive powers can be achieved. The required power for the connected loads can be effectively delivered and supplied by the proposed PV system and energy storage systems, subject to an appropriate control method. The ultimate goal of any power system is to maintain a balance between demand and supply of active power at any set point in time. Controllers integrating energy sources respond to the received signals and attempt to fulfil the grid demand. The system response is almost instantaneous and thus can be very helpful in grid frequency and voltage support. The grid voltage harmonic generation influences the PI current controller and generates current harmonics; the used harmonic compensator is effective for both positive and negative sequence fifth and seventh harmonics. The proposed control system is validated by means of simulation results.**

Keywords: *microgrid, PV source, energy storage, harmonic compensator, power quality.*

I. INTRODUCTION

The introduction of renewable energy sources (RES) is associated with the development of distributed power generating systems. The classical energy unidirectional distribution grid is replaced with a smart grid containing a multitude of microgrids (MGs), using RES and loads where the energy flow is bidirectional in respect with the main Grid. The control of the issues related to the stability of supply and energy quality in such grids are falling in the responsibility of the automated MGs, because the exponential increase of the control complexity makes not anymore possible the human dispatcher to perform it. From this point of view the RES have to participate to the quality control issues [1], [2]. This responsibility will be shared by sources and customers (loads) in the grid. In this way the dynamic stability of the MG has to be sustained by the RES power plant, too. One of the RES, the PV source, has, due to the electronic converters implied in its structure, the greatest answer speed capability to face with the stability problems, part of which are created in large extent by its own inherent variability of energy production. The premise used until now, to maximize the energy production using the maximum power point tracking (MPPT), will be replaced by the request to participate to the MG's operational stability [3-4]. This will mean to keep some part of the rated power as a reserve to be exploited in case of need. Also that request will require an associated energy storage facility besides the PV power plant. The difference between the PV power generation and local load consumption being directed to or supplied by the battery energy storage system connected via the power electronic interface. In our study we are starting to create a PV system on which study and, later, experiment some issues related to the dynamic stability and power quality of an MG supplied by a PV power plant. We will present aspects related not only on the grid connected MG, but to the possibility to operate it in an islanded way, too.

The system considered in the present study consists of a PV plant of 5.2 kW rated power, a battery banks (48V/100 Ah), a 5 kW three-phase VSI used to interface the DC-link to the grid through an LC filter. The simplified block diagram of the proposed system is shown in Fig 1.

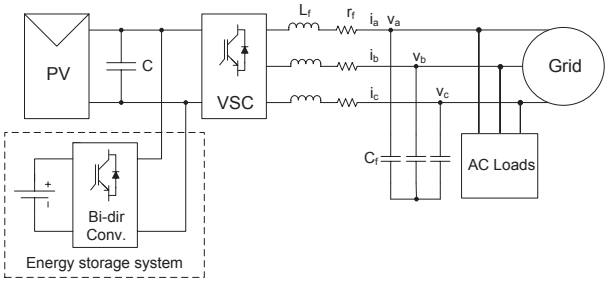

Fig. 1. Block diagram of analyzed system.

There are a lot of researches developed around the PV based MGs. Many of them are building around the same system adopted by us, [5]-[8], or without the storage facility, [9]. The dynamic control of the power supply to the grid and the stability of the MG related to the stability of grid in case of transients are at the beginning in many aspects as it can arise from the review papers such us [10]-[12].

The main objective of the present work is to implement a structure for improving the power quality and controllability of PV power plants for MG integration by means of

This work was supported by a grant of the Romanian National Authority for Scientific Research and Innovation, CNCS – UEFISCDI, project number PN-II-RU-TE-2014-4-0359.

energy storage system. The paper is organized as follows: in Section II the system configuration with the control methods, Section III describes the simulation results while the main conclusions are provided in Section IV.

II. System Configuration and Control

The analyzed PV power plant consists on 1 string of 22 series panels (≈ 5200 W) directly to the VSI DC-link, the rated DC voltage produced by the string being around 650V_{DC}. The PV panel's model is detailed in [13] and the datasheet parameters are given in [14]. The energy storage system consists of a storage element, in this case a bank of batteries and a bidirectional converter.

The lead acid batteries are the dominant energy storage technology, with their advantages of low price, high-unit voltage, stable performance and a wide operating temperature range [15], [16].

The battery bank consists of four 12 V batteries connected in series. The battery is able to supplement the power provided to the load by the PV, when the irradiation is too low. Batteries are the storage devices which cannot be overcharged or depleted completely. Their charging /discharging have to be controlled in order to maintain it for longer life. This care can be taken while generating the capability. For battery state of charge (SOC) estimation, the control method updated the SOC variable from one time step to the next, based on the power that goes through the cell stack. The control algorithm uses two variable parameters (I_{Batt}, V_{Batt}) and one constant block (c). With a discrete time–integrator block by accumulation the SOC is thus computed each cycle based on the previous SOC, depending on the input values. The change in SOC is implemented as follows:

$$SOC_{t+1} = SOC_t + \Delta SOC \tag{1}$$

$$\Delta SOC = \frac{\Delta E}{E_{capacity}} = \frac{P_{LAB} \cdot Time_{Step}}{E_{capacity}} = \frac{I_{Batt} \cdot V_{Batt} \cdot Time_{Step}}{P_{rating} \cdot Time_{rating}} \tag{2}$$

The basic principle of an SOC indication system is shown in Fig. 2.

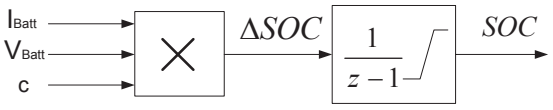

Fig. 2. Simplified battery SOC control method.

$$c = \frac{Time_{Step}}{P_{rating} \cdot Time_{rating}} = \frac{100 \cdot 10^{-6}}{5000 \cdot 4 \cdot 3600} \tag{3}$$

Where the values in (3) are corresponding to the practical studied system, the battery thus modeled is integrated in parallel with the DC link via the bidirectional DC-DC converter.

The bidirectional charge controller provides suitable charging conditions and regulates the current flow to avoid overcharge for battery protection. Connecting the battery through a DC–DC converter provides flexibility in choosing the DC-link voltage level, and the battery voltage and configuration. It also enables the battery to provide the necessary power to maintain a constant load voltage.

The simplified layout of the bidirectional charge controller is presented in Fig. 3. This control algorithm uses a constant DC reference voltage (V_{DC_ref}) to charge/discharge a battery.

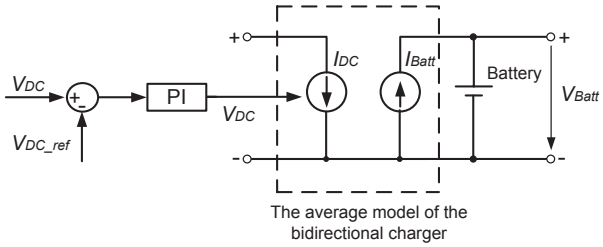

Fig. 3. The control mode of the bidirectional charge controller.

The DC voltage (V_{DC}) is compared with a reference voltage (V_{DC_ref}) and an error signal is obtained. With a PI (proportional-integrator) controller, the DC value of the charge/discharge current (I_{DC}) is obtained. When $I_{DC} > 0$ the battery is charging, and when $I_{DC} < 0$ the battery is discharging. It measures the power output of the PV system and the state of charge (SOC) of the battery and decides how much energy can be delivered/absorbed at a given moment.

A 5000 μF capacitor is considered on the DC-link of the PV battery system. The 5 kW three-phase VSI is responsible for converting the DC power from the PV-battery system into AC mains power and feeds it into the grid.

The whole system was sized to ensure the adequate output for the load and to the grid. The PWM of the inverter and the LC filter (L_f =2 mH, C_f =10 μF) was adequately sized to reduce the THD under the standard value. To have the desired reference AC currents at the output, the magnitude and phase information is essential.

A simple PI loop generates the magnitude of the current by comparing the DC link voltage to the reference value, and a phase locked loop provides the voltage phase angle information. Thus PI controller takes care of the voltage at the DC bus. The controller generates a positive reference current for a positive error and a negative reference current for a negative error.

The control structure of the grid side converter based on PI current controllers in *dq* frame is presented in Fig. 4. The i_q current component determines reactive power while i_d decide the active power flow.

The input of the current controller is the error between the measured and reference grid current. The current controller output is the reference grid voltage, which divided by the DC source voltage gives the duty cycle for the inverter. The power quality problem of the power supplied by the PV-battery source is related to the harmonics content of the AC wave generated by the inverter.

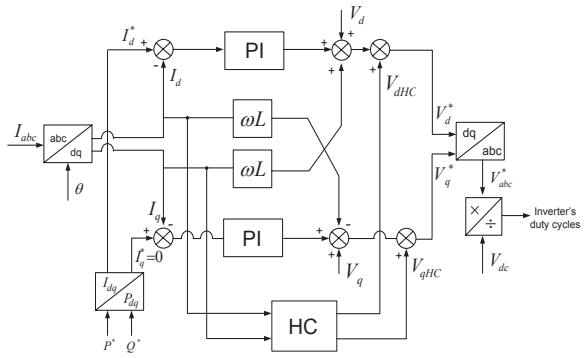

Fig. 4. The dq current control based on PI controller with HC.

In order to reduce the harmonics content, expressed by the THD, a supplementary Harmonics Compensator (HC) is applied in synchronous reference frames, where the currents being regulated are DC quantities, which eliminates the steady-state error, in order to obtain an improved power quality in the analyzed configuration.

Among numerous current control schemes reported in the literature [17]-[19], in the studied HC control structure (Fig. 5) two controllers are implemented in two frames rotating at -5ω and +7ω, one frame for each harmonics. As the most important harmonics in the current spectrum are the 5th and 7th, in this paper HC is designed to compensate these two selected harmonics.

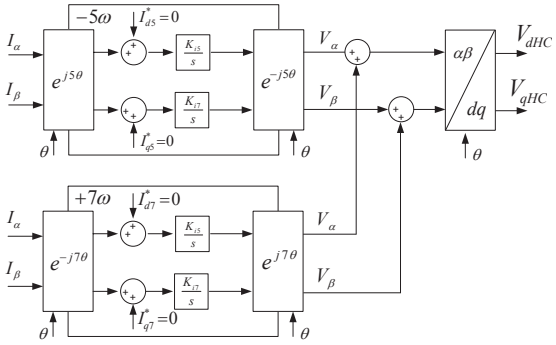

Fig. 5. The HC diagram for PI controller.

In order to synchronize the grid connected VSI and control of injected current to ensure unity power factor at point of common coupling (PCC), a PLL block is used. Also, PLL system can be used to detect the frequency and phase of the harmonics in order to select the proper speed of the synchronous frame. The implemented PLL structure in our analyzed control structure is based on [21], where the positive-sequence voltage vector is translated from the αβ stationary reference frame to the *dq* rotating reference frame by means of Park's transformation.

III. Simulation Results

The proposed PV-battery MG system has been modeled and simulated using the Matlab/Simulink environment. Fig. 6 presents the Simulink diagram of the PV-battery connected to the MG by means of a three-phase inverter.

In order to investigate the system's operation, the system is tested under different scenarios to show that operation is quick enough in response to the commanded signals. The system is tested in the synchronous *dq*-PI, for two different cases as follows:

- constant reference inverter power (P_{inv}=*3 kW*) and constant AC loads (P_{load} = *5 kW*), with harmonic generation, without and with HC for variable irradiation PV levels.

- step change in the inverter power reference for 3 kW to 5 kW at t=3 s and variable AC loads (see Fig. 16 – green line), with harmonic generation, without and with HC for a constant PV irradiation level.

The following figures show the simulation results followed by a discussion about improving the power quality and controllability of PV power plants for microgrids integration by means of energy storage system.

A. Case 1: PV-battery system variation at constant local load

In the first case, a variation in the PV irradiation was applied, (see Fig. 7) in order to simulate a real PV operating condition. The simulations were performed at 3 kW constant inverter reference power value and 5 kW total load power demand. The reactive power reference is set to zero.

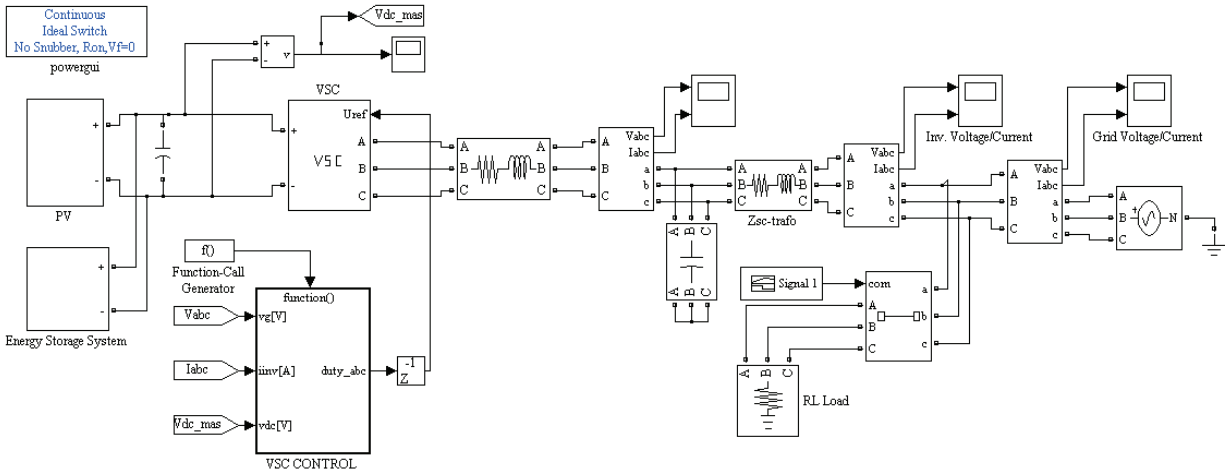

Fig. 6. Simulink diagram of the studied system.

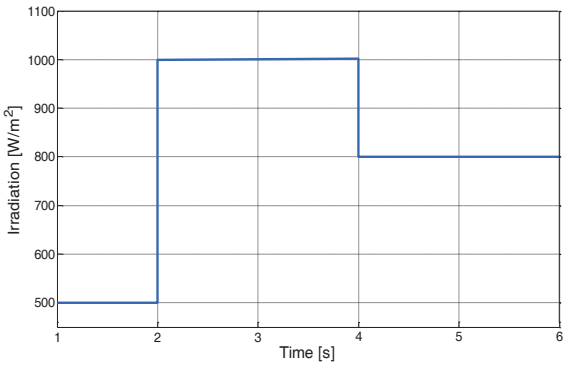

Fig. 7. Variable irradiation of PV array input.

By using a PI regulator, the DC inverter voltage link, presented in Fig. 8, is maintained around 650 V_{DC} according to the PV irradiation levels. For testing the effectiveness of HC, a 5th and 7th harmonic order injection by the three phase voltage grid is applied into the system for whole duration of the simulation.

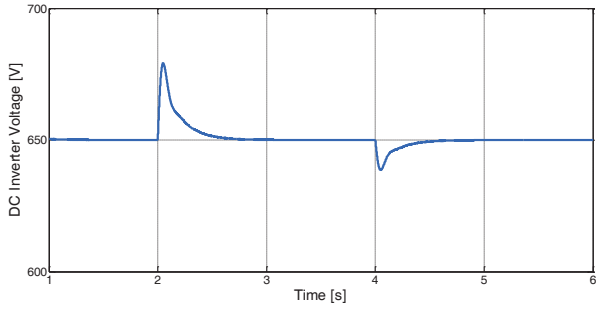

Fig. 8. DC inverter voltage link variation.

In Fig. 9, during this process, the negative current implies that the battery is in discharging mode. When the battery is charging, the battery voltage increases by about 2 V (at t=2 s for 1000 W/m^2) and decreases by about 1 V (starting with t=4 s for 800 W/m^2).

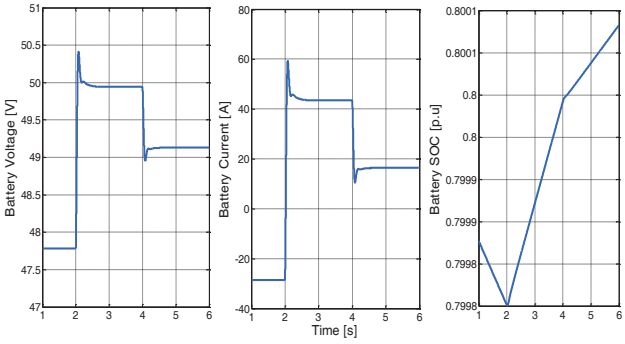

Fig. 9. Battery voltage, current and SOC variation.

The initial battery SOC is considered 80 %. In the transient regime, the battery SOC passes from discharging to charging mode in order to ensure the stability of the supply for the loads.

As it can be seen in Fig. 10, at 500 W/m^2, the power produced by the PV system cannot supply the entire load energy demand (5 kW), therefore the battery will supply the difference.

The excess power (at 1000 W/m^2) is stored in the battery bank. Consequently, Fig. 10 shows that the power balance of the PV-battery system is maintained.

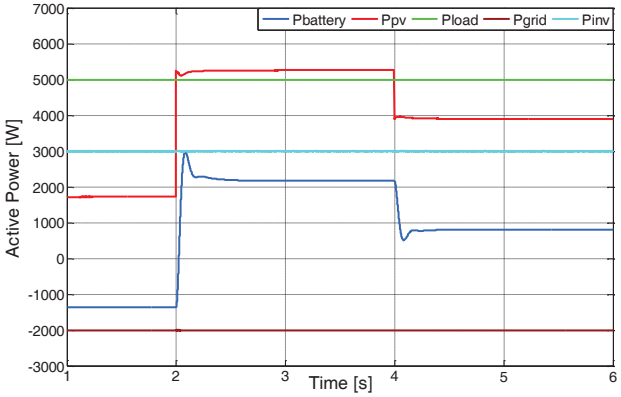

Fig. 10 Active power balance in the PV-battery system.

The grid currents variation waveforms without/with HC are presented in Fig. 11.

According to [20] the injected current and voltage in the grid should not have a THD larger than 5 % (for current) and 8 % (for voltage). The FFT analysis was made for 3 kW inverter active power reference value to obtain the graphical representation of the harmonic spectrum for phase A (I_a) with harmonic injection in both cases: without and with HC starting at t= 5.08 s for 1 cycle.

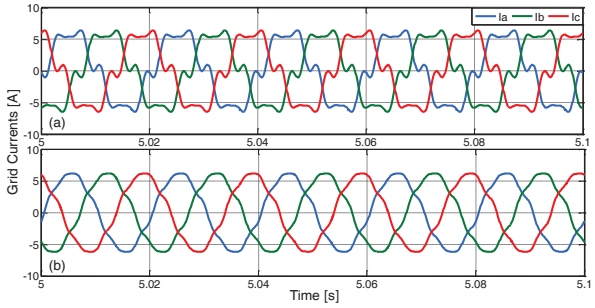

Fig. 11. Grid currents variation: (a) without HC; (b) with HC.

The grid currents THD containing the 5th and 7th harmonics are processed in Matlab/Simulink with a Powergui block.

As can be seen in Fig. 12, when is applied a harmonic injection is enabled (i.e. the grid has harmonic components), without HC, the level of THD current is 23.26 % for 3 kW inverter power reference. After the HC activation, the THD level decreases at 6.00 %.

By compensating the 5th and 7th harmonics, the THD current is drastically reduced, while the PI-HC controller implemented in *dq* frame having good performances at partial powers representing 60 % of the rated value (5 kW).

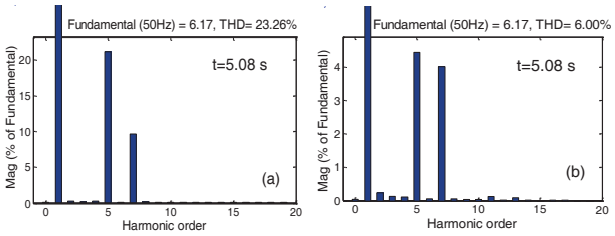

Fig. 12. Grid current (I_a) harmonic spectrum: (a) without HC; (b) with HC.

The measured grid voltages variation with harmonic injection is shown in Fig. 13. In Fig 14, the resulted voltage THD (5.91 %) calculated for 1 cycle starting at t=5.08 s is in accordance with the standards.

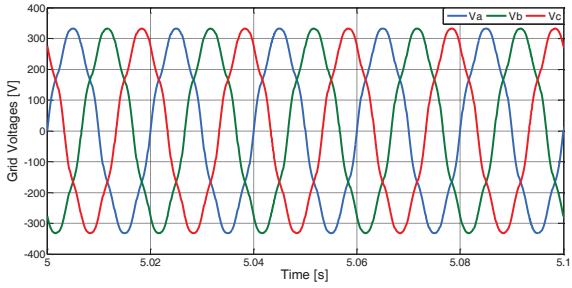

Fig. 13. Grid voltages variation with harmonic injection.

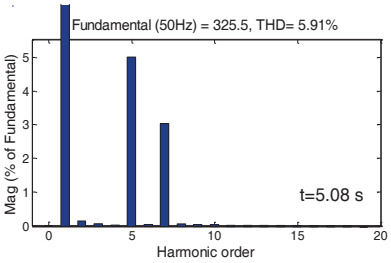

Fig. 14. Grid voltage (V_a) harmonic spectrum with harmonic generation content

B. *Case 2: PV-battery system variation at variable local load*

In order to test again the transient performance of the proposed PV-battery control method, a variation of the full power load demand is considered (at t=2 s, a 5 kW load is connected and disconnected at t=4 s) for a constant PV irradiation level (1000 W/m^2). Also, a step change in the inverter power reference from 3 kW to 5 kW at t=3 s is applied. The battery voltage, current and SOC variation results are presented in Fig. 15. For this case, the battery is in charging mode for the whole duration of the simulation. Until the load is connected, all the power produced by PV plant is stored in the battery. Also, at t=2s when a 5 kW local load is connected, the PV ensure stable supply for the loads (the approximately 0.2 kW excess power is stored in the battery), and the battery charging mode is maintained during the transient event. When the inverter power is changed, the battery voltage decreases by about 1.5 V (at t=3 s), and the positive current implies that the battery remains in charging process.

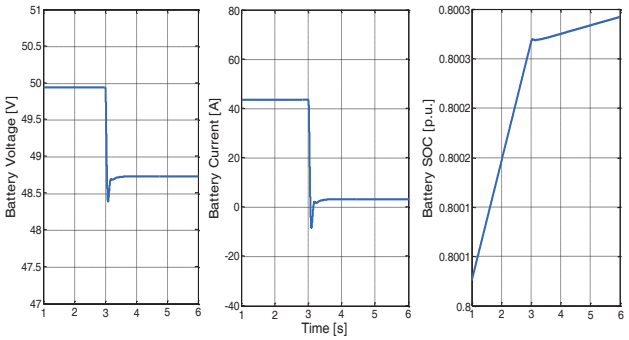

Fig. 15. Battery voltage, current and SOC variation.

The case of VSI output power increasing from 3000W up to around 5000W is shown in Fig. 16, which highlights the power balance of the PV-battery connected to the grid system.

A good transient behavior of the PI controller can be noticed in this situation. The current is controlled according to its new reference and the output power of the VSI smoothly reaches its new operating point. These results confirm that the proposed control algorithm is stable, achieving zero steady-state error at fundamental frequency and having a good transient response. A zoom in the grid currents starting at t=5s in both situations without/with HC can be seen in Fig. 17.

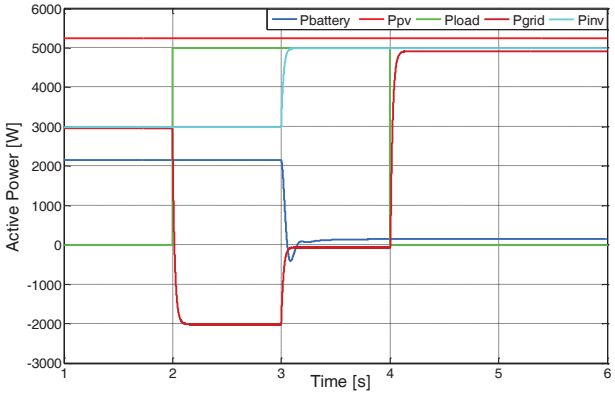

Fig. 16. Active power balance in the PV – battery system.

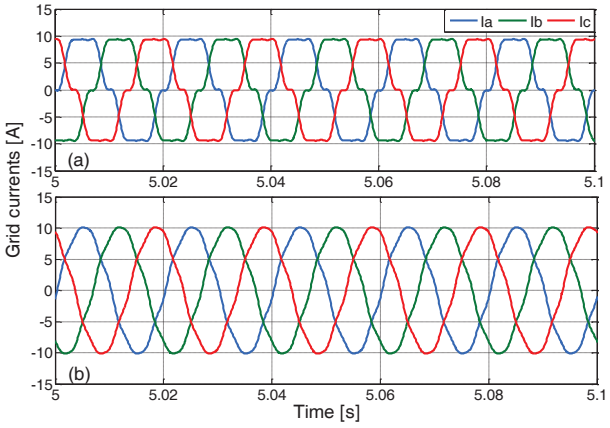

Fig. 17. Grid currents variation: (a) without HC; (b) with HC.

As can be seen in Fig. 18, when a harmonic injection is applied, without HC, the level of THD current is 14.21 % for 5 kW, while after HC implementation, the THD level decreases at 3.78 % and the system is within the standards at rated power.

The grid voltages are balanced and unaffected by the step change in the inverter power reference for 3 kW to 5 kW and the grid voltage THD is similar by the previously case (see Fig. 13 and Fig. 14).

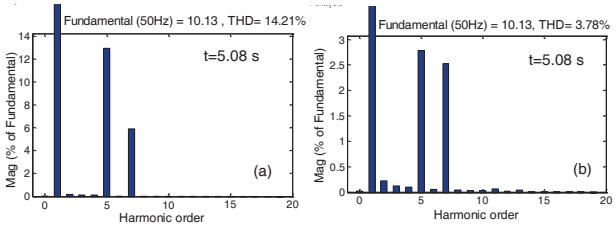

Fig. 18. Grid current (I_a) harmonic spectrum: (a) without HC; (b) with HC.

IV. CONCLUSIONS

The behaviour of an interfacing system for improving power quality and controllability of PV power plants for MG integration has been presented in this paper.

This includes an associated energy storage system facility in the PV DC link besides the PV power plants with the role to enhancing the control for MG integration. A *dq*-PI control strategy has been applied in order to design a current controller for grid-connected VSI, with the main focus on harmonics distortion and tracking performance. The control strategies are performing well under normal and transient PV irradiation conditions.

The analyzed two cases were provided in terms of the harmonic generation dependent on the PI controller structure without and with HC for constant and variable loads.

With harmonic injection and without HC, the system does not comply with the IEEE 1547.2 standard in terms of harmonic content. By compensating the 5th and 7th harmonics, the system is within the standards, at rated power and at partial powers representing 60 % from the rated value. Stair change in the PV power shows good battery response in the case of increase/decrease in load.

The simulations results show that the enhance control method ensures good effectiveness in meeting the stringent grid harmonic standard it is suitable for MG integration.

Received on July 18, 2016
Editorial Approval on November 11, 2016

REFERENCES

[1] A. Choudar, D. Boukhetala, S. Barkat, J.M Brucker, "A local energy management of a hybrid PV-storage based distributed generation for microgrids", *Energy Conversion and Management*, vol. 90, 2015, pp. 21–33.

[2] J. M. Guerrero, P. C. Loh, T.-L. Lee, and M. Chandorkar, "Advanced control architectures for intelligent microgrids—Part II: Power quality, energy storage, and ac/dc microgrids", *IEEE Transaction on Industrial Electronics*, vol. 60, no. 4, Apr. 2013, pp. 1263, 1270.

[3] S-T Kim, S. Bae, Y. C. Kang and J-W Park, "Energy management based on the photovoltaic HPCS with an energy storage device", *IEEE Transactions on Industrial Electronics*, vol. 62, no. 7, July 2015, pp. 4608-4617.

[4] Y. Guan, J. C. Vasquez, J. M. Guerrero, Y. Wang, and W. Feng, "Frequency stability of hierarchically controlled hybrid photovoltaic-battery-hydropower microgrids", *IEEE Transactions on Industry Applications*, vol. 51, no. 6, Nov. 2015, pp. 4729-4742.

[5] J. Quesadaa, R. Sebastiánb, M. Castrob, J.A. Sainz, "Control of inverters in a low voltage microgrid with distributed battery energy storage. Part I: Primary control", *Electric Power Systems Research*, vol. 114, 2014, pp. 126–135.

[6] T. L. Vandoorn, J. D.M. De Kooning, B. Meersman, B. Zwaenepoel, "Control of storage elements in an islanded microgrid with voltage-based control of DG units and loads", *Electrical Power and Energy Systems*, vol. 64, 2015, pp. 996–1006.

[7] H. Mahmood, D. Michaelson, and J. Jiang, "A power management strategy for PV/battery hybrid systems in islanded microgrids", *IEEE Journal of Emerging and Selected Topics in Power Electronics*, vol. 2, no. 4, Dec. 2014, pp. 870-882.

[8] S. Gaurava, C. Birlaa, A. Lambaa, S. Umashankara, S. Ganesanb, "Energy management of PV-battery based microgrid system", *Procedia Technology*, vol. 21, 2015, pp. 103 – 111.

[9] M. Mahzarnia, A. Sheikholeslami, "Improvement the dynamic voltage profile by a voltage stabilizer in microgrids with a type of inverter based resource", *Intelligent Systems and Applications Journal*, 2013, pp. 39-46.

[10] F.M Uriarte, C. Smith, S. VanBroekhoven, R.E. Hebner, "Microgrid ramp rates and the inertial stability margin", *IEEE Transaction on Power Systems*, vol. 30, no.6, Nov. 2015, pp. 3209-3216.

[11] J.G de Matos, F. S.F.e Silva, L.A.de S Ribeiro, "Power control in ac isolated microgrids with renewable energy sources and energy storage systems", *IEEE Transaction on Industrial Electronics*, vol.62, no.6, June 2015, pp.3490-3498.

[12] S. Parhizi, H. Lotfi, A. Khodaei, S. Bahramirad, "State of the art in research on microgrids: a review", IEEE *Access*, vol. 3, 2015, pp.890-925.

[13] L. Barote, C. Marinescu, "Renewable Hybrid System with Battery Storage for Safe Loads Supply", *IEEE PowerTech*, 19 - 23 June 2011, Trondheim, Norway, pp. 1-5.

[14] Poly-crystaline solar panel 200-250 W, http://www.risenenergy.com.

[15] C.A. Hill, M.C. Such, D. Chen, J. Gonzalez and W.M. Grady, "Battery energy storage for enabling integration of distributed solar power generation", *IEEE Transactions on Smart Grid*, vol. 3, no. 2, June 2012, pp.850 - 857.

[16] M. T. Lawder, V. Viswanathan, V. R. Subramanian, "Balancing autonomy and utilization of solar power and battery storage for demand based microgrids", *Journal of Power Sources*, vol. 279, 2015, pp. 645-655.

[17] R. Teodorescu, M. Liserre and P. Rodríguez, "Grid converters for photovoltaic and wind power systems", *John Wiley & Sons, Ltd, Publication*, 2011.

[18] J. Rocabert, A. Luna, F. Blaabjerg, P. Rodriguez, "Control of power converters in ac microgrids", *IEEE Transaction on Power Electronics*, vol.27, no.11, Nov. 2012, pp. 4734-4748.

[19] I. Serban, C. Marinescu, "Control strategy of three-phase battery energy storage systems for frequency support in microgrids and with uninterrupted supply of local loads", *IEEE Transaction on Power Electronics*, vol. 29, no. 9, Sept. 2014, pp 5010-5021.

[20] *** IEEE 1547.2-2008, "IEEE standard for interconnecting distributed resources with electric power systems", 2009.

[21] N. Jaalam, N.A. Rahim, A.H.A. Bakar, C. Tan, A.M.A. Haidar, "A comprehensive review of synchronization methods for grid-connected converters of renewable energy source", *Renewable and Sustainable Energy Reviews*, vol. 59, 2016, pp. 1471–1481.